



This is a repository copy of *Sensitivity analysis of a model of lower limb haemodynamics*.

White Rose Research Online URL for this paper:

<https://eprints.whiterose.ac.uk/189720/>

Version: Accepted Version

---

**Proceedings Paper:**

Otta, M., Halliday, I., Tsui, J. et al. (3 more authors) (2022) Sensitivity analysis of a model of lower limb haemodynamics. In: Groen, D., de Mulatier, C., Krzhizhanovskaya, V.V., Sloot, P.M.A., Paszynski, M. and Dongarra, J.J., (eds.) Computational Science – ICCS 2022 : 22nd International Conference, London, UK, June 21–23, 2022, Proceedings, Part III. 22nd International Conference on Computational Science – ICCS 2022, 21-23 Jun 2022, London, UK. Lecture Notes in Computer Science (13352). Springer International Publishing , pp. 65-77. ISBN 9783031087561

[https://doi.org/10.1007/978-3-031-08757-8\\_7](https://doi.org/10.1007/978-3-031-08757-8_7)

---

This is a post-peer-review, pre-copyedit version of a paper published in Lecture Notes in Computer Science. The final authenticated version is available online at:  
[http://dx.doi.org/10.1007/978-3-031-08757-8\\_7](http://dx.doi.org/10.1007/978-3-031-08757-8_7).

**Reuse**

Items deposited in White Rose Research Online are protected by copyright, with all rights reserved unless indicated otherwise. They may be downloaded and/or printed for private study, or other acts as permitted by national copyright laws. The publisher or other rights holders may allow further reproduction and re-use of the full text version. This is indicated by the licence information on the White Rose Research Online record for the item.

**Takedown**

If you consider content in White Rose Research Online to be in breach of UK law, please notify us by emailing [eprints@whiterose.ac.uk](mailto:eprints@whiterose.ac.uk) including the URL of the record and the reason for the withdrawal request.



[eprints@whiterose.ac.uk](mailto:eprints@whiterose.ac.uk)  
<https://eprints.whiterose.ac.uk/>

# Sensitivity analysis of a model of lower limb haemodynamics

M Otta<sup>1,2,3</sup>[0000-0002-8062-1354], I Halliday<sup>2,3</sup>, J Tsui<sup>4,5</sup>, C Lim<sup>4</sup>, Z R Struzik<sup>1,6,7</sup>[0000-0002-1352-8897], and A Narracott<sup>2,3</sup>[0000-0002-3068-6192]

<sup>1</sup> Sano Centre for Computational Medicine, Modelling and Simulation Research Team, Czarnowiejska 36, building C5, 30-054 Kraków, Poland (<https://sano.science/>)

<sup>2</sup> Department of Infection, Immunity and Cardiovascular disease, University of Sheffield, Sheffield, UK

[motta1@sheffield.ac.uk](mailto:motta1@sheffield.ac.uk)

<sup>3</sup> Insigneo Institute for *in silico* medicine, University of Sheffield, Sheffield, UK

<sup>4</sup> University College London, London, UK

<sup>5</sup> Royal Free London NHS Foundation Trust, London, UK

<sup>6</sup> Faculty of Physics, University of Warsaw, Pasteura 5, 02-093 Warsaw, Poland

<sup>7</sup> Graduate School of Education, The University of Tokyo, 7-3-1 Hongo, Bunkyo-ku, Tokyo 113-0033, Japan

**Abstract.** *Post-thrombotic syndrome (PTS) has variable clinical presentation with significant treatment costs and gaps in the evidence-base to support clinical decision making. The contribution of variations in venous anatomy to the risk of complications following treatment has yet to be characterized in detail. We report the development of a steady-state, 0D model of venous anatomy of the lower limb and assessments of local sensitivity (10% radius variation) and global sensitivity (50% radius variation) of the resulting flows to variability in venous anatomy. An analysis of orthogonal sensitivity was also performed. Local sensitivity analysis was repeated with four degrees of thrombosis in the left common iliac vein. The largest normalised sensitivities were observed in locations associated with the venous return. Both local and global approaches provided similar ranking of input parameters responsible for the variation of flow in a vessel where thrombosis is typically observed. When a thrombus was included in the model increase in absolute sensitivity was observed in the leg affected by the thrombosis. These results can be used to inform model reduction strategies and to target clinical data collection.*

**Keywords:** Post-thrombotic Syndrome · Venous model · Sensitivity analysis.

## 1 Introduction

Deep vein thrombosis (DVT) of the lower limb is a health condition in which blood clots form in deep veins of the leg due to some pathological changes of the blood vessels or the blood itself [1]. It is estimated to affect 1-2 per 1,000 people each year and between 20 and 50% of them will develop long term complications known as post-thrombotic syndrome, PTS [2, 3]. The condition is not terminal, but it significantly impairs quality of life. The highly variable clinical presentation of PTS makes it difficult to treat and, due to extensive follow-up and repeat medical interventions, treatment pathways are associated with significant cost. The placement of a stent, a metallic scaffold used to restore the vessel diameter following disease, has increased in recent years [4], but there are significant gaps in the evidence-base to support clinical decision making around use of stents [5]. The contribution of venous anatomy to variation in blood flow in the region of the thrombosis and resulting risk of complications following stent placement has yet to be characterized in detail.

Reduced order modelling approaches using one dimensional (1D) and zero dimensional (0D) formulations to characterise pressure-flow distributions in blood vessels have been extensively reported in the literature, particularly in the context of research questions associated with the arterial circulation [6]. A 1D formulation considers continuous variation of variables along the circulation, whereas a 0D approach, also known as lumped-parameter, or compartmental modelling, represents elements of the circulation as lumped compartments. The status, challenges and prospects of the 0D method, again with emphasis on arterial applications, was recently provided by Hose et al. [13]. There have been relatively few studies which focus on the venous circulation, of particular note in the context of this study are reports by Müller and Toro [7] who describe a 1D model of both the arterial and venous circulation, with focus on the cerebral vasculature and Keijsers et al. [8] who employed a 1D formulation to study the interaction between the venous circulation in the lower limb and the activity of the calf muscle pump.

The assessment of model sensitivity and the quantification of the propagation of uncertainty from model inputs to model outputs has become acknowledged as an essential aspect of model development, particularly when model outputs are used to inform clinical decision making [9] or to identify biomarkers of disease states [10]. However, uncertainty quantification is often computationally expensive and is not always performed during the development of new modelling approaches. More complex models frequently lack sensitivity analysis.

This study reports the development of a model of venous haemodynamics with focus on the influence of variation in the venous anatomy on the distribution of flow within the veins of the lower limb. This represents the first step towards modelling venous flow of the lower limb to aid clinical decision making in treatment of PTS. The approach uses data reported by Müller and Toro [7] to characterise the lower limb circulation, combining this with a local and global sensitivity analysis.

## 2 Methods

This section summarises construction of the model under investigation followed by a description of the sensitivity analyses performed. The application of local and global sensitivity analyses to the venous network without thrombosis is described. This is followed by assessment of the change in local sensitivity of the network following the development of a thrombus. All analyses were performed using Python, using libraries including `numpy` and `pandas` to manipulate data and to solve the model, `matplotlib` to visualise results, and `SALib` to perform global sensitivity analysis.

### 2.1 Lower limb circulation model

In this study a steady-state, 0D model was used to account for the complicated venous anatomy of the lower limb without considering the pulsatility of arterial or venous flow or vessel wall elasticity. The model topology and input parameters were taken from anatomical data reported by Müller and Toro (given in Table III, VI and VIII in [7]). The form of the model is shown in Figure 1.

The mean radius and length of each vessel were used to compute the corresponding Poiseuille resistance, given by equation (1).

$$R = \frac{8\mu L}{\pi r^4} \quad (1)$$

where  $\mu$  is the viscosity of blood,  $r$  is a radius representing the cross section of the considered vessel and  $L$  is its length.

To simplify the form of the model, where vessels were arranged in series in the vascular network, they were represented as a single resistive element. The arterial circulation was taken to start at the abdominal aorta (representing flow into the lower limb only) and three pathways were considered to contribute to venous return to the heart (the inferior vena cava, the azygos vein and the vertebral venous plexus). The full model consisted of 50 resistances (15 arterial, 8 capillary beds, 27 venous) informed by 42 input vessel radii and length parameters. The boundary conditions to the model consisted of the pressure gradient between the abdominal aorta and the venous return to the heart. The aortic pressure was set to 80mmHg and the pressure at all outlets was assumed to be zero.

Vessel properties were assigned to the elements of the model, based on a prepared text file with one column listing these elements and another column listing all contributing vessel properties, to account for some of them being lumped into a single resistor. The resistance between the arterial and venous system was calculated by summing the resistance of arterioles, capillaries and venules and their distal resistance as provided by Müller and Toro.

To simulate thrombosis, resistance of specific blood vessels was recalculated and replaced in the dataset based on a percentage reduction in the mean radius. A system of equations describing the model was constructed using Kirchhoffs'

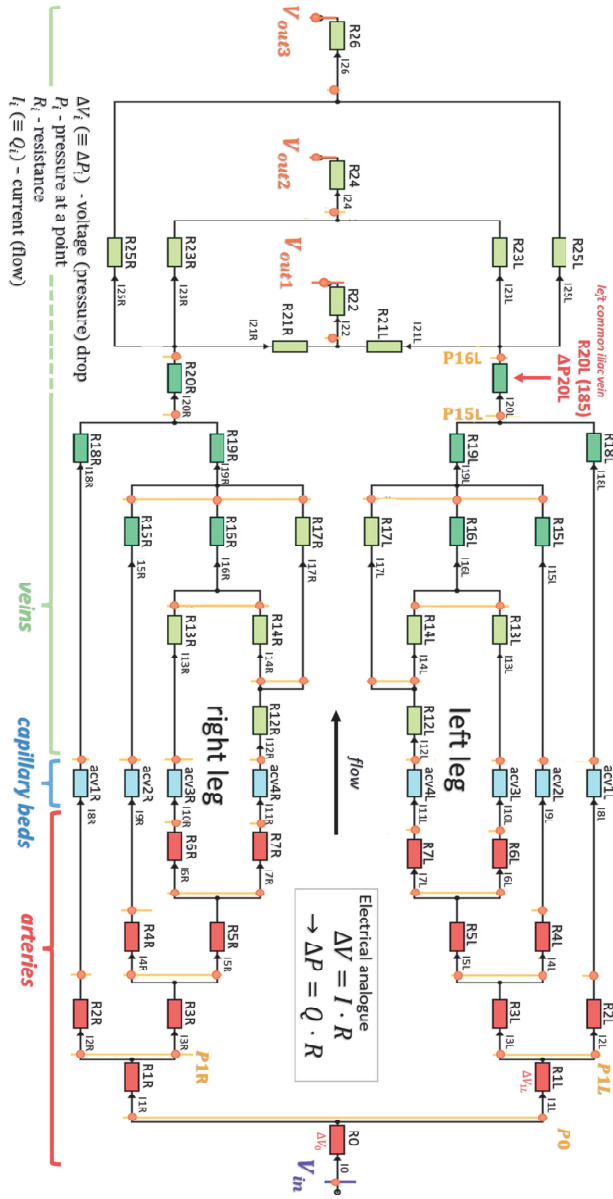


**Fig. 1.** Model formulation. Flow in the circulation is from right to left. Red elements represent large arteries, blue elements represent arterioles, capillaries and venules and green elements represent veins. All vessels are modelled as purely resistive elements.

laws. There are 30 unique pathways from inlet to outlet and the pressure drop along each must equal the specified boundary condition. At every junction, the sum of flows entering equals the sum of flows exiting that junction. This results in an overspecified system of 66 equations. A row-echelon reduction algorithm was implemented to reduce and solve the system. The solution of the model provides flow at all locations, which is then post-processed to provide the corresponding pressure everywhere in the model.

## 2.2 Sensitivity analysis

**Local sensitivity:** Local sensitivity indices are based upon the first-order partial derivative in (2), where  $y_i$  is the  $i^{th}$  output of the model,  $p_j$  is the  $j^{th}$  input parameter and  $\Delta p_j$  is a small perturbation in its value.

$$\frac{\partial y_i}{\partial p_j} = \lim_{\Delta p_j \rightarrow 0} \left( \frac{y_i(p_j + \Delta p_j) - y_i(p_j)}{\Delta p_j} \right) \quad (2)$$

Of course, all other input parameters  $p_k$ ,  $k \neq j$  are held constant when taking the above limit. Accordingly, parameter variation is designated OAT (*one at a time*), and takes place around a base state, representative of a given physiological state. For present purposes, the partial derivative in (2) is computed from the numerical quotient  $\frac{\Delta y_i}{\Delta p_j}$ , where  $\Delta y_i$  is the measured change in output  $y_i$ , caused by a change,  $\Delta p_j$ , in input parameter  $p_j$ , typically by a few percent. It is often convenient to contextualise this quotient, to account for the absolute value of  $y_i$  and  $p_j$ , as we describe shortly.

To assess the sensitivity of the model outputs to variability in venous anatomy a local sensitivity analysis was performed. Each of the 42 radii of the blood vessels was varied by  $\pm 10\%$  from the reference value in turn, with all other radii kept constant. The model was solved 3 times for each vessel, with  $r_{base}$  - the original value,  $r_{min} = 0.9 \cdot r_{base}$  and  $r_{max} = 1.1 \cdot r_{base}$ . This produced 3 sets of output flows,  $Q$ , for each of the 42 radii. It is important to note that because some vessels are lumped, two or three radii contribute to the same resistor.

Two matrices were constructed and compared to visualise the relationships between the change in radii ( $\Delta r$ ) with the resulting change in flows ( $\Delta Q$ ). The first was a matrix of absolute changes, with elements described by equation (3).

$$a_{ij} = \frac{\Delta Q_j}{\Delta r_i} = \frac{[Q_{max} - Q_{min}]_j}{[r_{max} - r_{min}]_i} \quad (3)$$

$Q_{max}$  corresponds to flows obtained by changing the radius of a vessel to  $r_{max}$ , and  $Q_{min}$  to  $r_{min}$ . Returning to the issue of contextualisation, our second matrix reports relative changes, with respect to the base values of the radii and flows, with elements described by equation (4). Changes  $\Delta Q$  and  $\Delta r$  are calculated in the same way as in equation (3).

$$s_{ij} = \frac{\left[\frac{\Delta Q}{Q}\right]_j}{\left[\frac{\Delta r}{r}\right]_i} \quad (4)$$

The left common iliac vein, a deep vein of the ilio-femoral region, is a likely place for thrombus development. In the Müller and Toro dataset it corresponds to the vessel no. 185 (resistor *R20L* in the current model) and is associated with flow *Q20L*. The relative influence of each input parameter on this flow value was evaluated using the sensitivity vector for this particular output value.

An analysis of orthogonal sensitivity was also performed. The vector in equation (5) expresses the relative sensitivity of all outputs (flows) to the  $i^{\text{th}}$  input (radius).

$$\underline{s}_i = (s_{i1}, s_{i2}, s_{i3}, \dots, s_{iN}). \quad (5)$$

The normalised inner product in equation (6) therefore measures the orthogonality (effective independence) of the  $i^{\text{th}}$  and  $j^{\text{th}}$  input parameters [11].

$$p_{ij} = \frac{\underline{s}_i \cdot \underline{s}_j}{|\underline{s}_i| \times |\underline{s}_j|}. \quad (6)$$

If the output scalar is close to  $\pm 1$ , the input parameter pair has a similar effect on the system, if it is close to zero, their effects are independent.

**Global sensitivity - Sobol analysis:** Global sensitivity analysis differs from the local approach in that (i) all input parameters are varied (i.e. we no longer change input parameters OAT) and (ii) outputs (in contradistinction to their rates of change with respect to inputs) are considered directly. The type of analysis performed was the Sobol sensitivity analysis, which is based on variance decomposition. It allows one to measure the contributions of model inputs to variance of model outputs. First-order indices inform relative influence of every input, second order indices measure the contributions of the interactions between two input parameters, and so on [12].

The programming language used was Python with SALib library - following a procedure described in the SALib documentation. Interactions of first and second order were investigated. Ranges for parameter variation were set to  $\pm 50\%$  from their nominal values. Data points were sampled from Saltelli sequence for six cases,  $n = \{1, 3, 5, 7, 10\}$ , with  $2^n$  being an input to `sobol.saltelli()` function related to the number of samples,  $N_s$ . The specific relationship between  $n$  and  $N_s$  depends on the order of Sobol indices included in the analysis. For the case investigated, the smallest set of samples  $N_s = 216$ , and the biggest  $N_s = 110,592$ . Each sample is a 42-dimensional vector generating a 50-dimensional output flow vector. For each output, the vector containing the value of that output for all samples was provided to the `sobol.analyze()` function which

returns a dictionary of Sobol indices and their confidence values. Convergence of first-order indices was checked to validate the sample size. The case of  $n = 10$  was chosen for further analysis.

A matrix of first-order interactions between inputs and outputs as well as the corresponding confidence matrix were constructed to identify parameters of significant influence. Second-order interactions were first investigated by binning and assessing their index and confidence values for all parameter pairs. For each of the 50 output flows, a matrix of parameter interactions was constructed to identify interactions significant to the output variance.

**Influence of thrombus formation:** Four different degrees of thrombosis were introduced to the left common iliac vein (no. 185) by reducing its radius, in turn, by 30%, 40%, 50% and 60%. A local sensitivity matrix was constructed for each case, for  $\pm 10\%$  changes to every radius, and compared to the original absolute sensitivity matrix for the no-thrombus case.

### 3 Results

This section summarises results obtained from the analysis of local sensitivity (varying one parameter at a time) and global sensitivity (varying all parameters simultaneously), as well as the influence of thrombus formation on absolute local sensitivity.

**Local sensitivity:** A comparison of absolute and normalised (relative) sensitivity matrices is shown in Fig. 2. Input and output parameters corresponding to cells of highest and lowest sensitivity value are highlighted in yellow.

The two matrices vary in that the most significant radii in the absolute sensitivity belong to veins in the middle of the model, whereas for relative sensitivity, vessels close to the venous return appear to be more significant. It is worth noting that cells of highest values in the absolute sensitivity matrix are still significant in the relative sensitivity matrix, but not as much as those in the bottom right corner.

Ranked normalised sensitivity for flow  $Q_{20L}$  is shown in Fig. 3. This is a flow in left common iliac vein - a potential site of thrombosis. Out of 42 radii, 13 display influence on the flow and the first 5 belong to the arterial network of the left leg.

The distribution of inner product values and a heatmap of their absolute values are presented in Fig. 4. This distribution has a clear peak at zero, demonstrating that many of the sensitivity vectors are independent of one another. The clustering of entries close to  $-1$  and  $1$  represent parameters which induce similar response of the system.

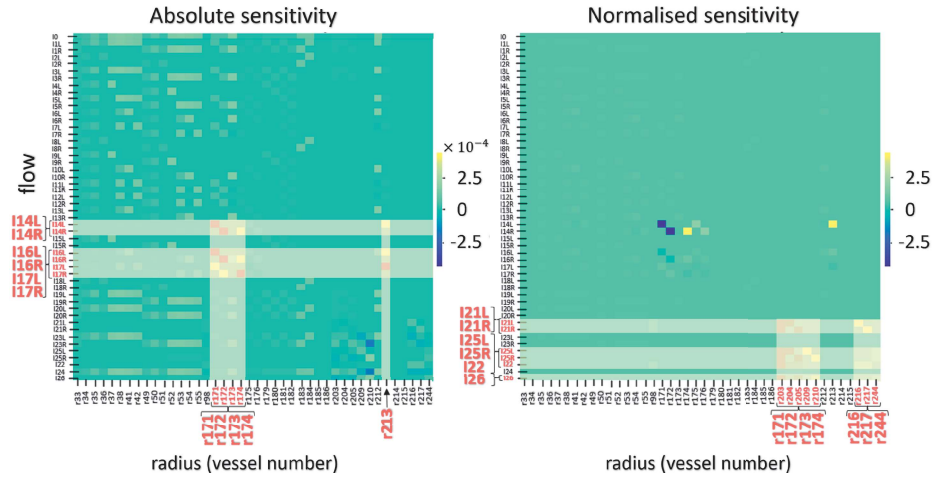


**Fig. 2.** Absolute vs normalised sensitivity. The most sensitive parameters and outputs are highlighted in both figures. Colour scales are adjusted such that distinctive features of both matrices are visible.

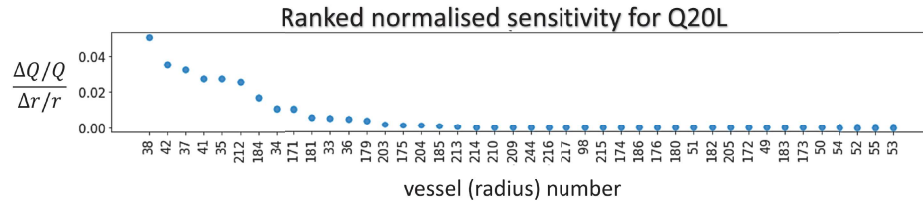


**Fig. 3.** Relative influence of input parameters on Q20L flow.

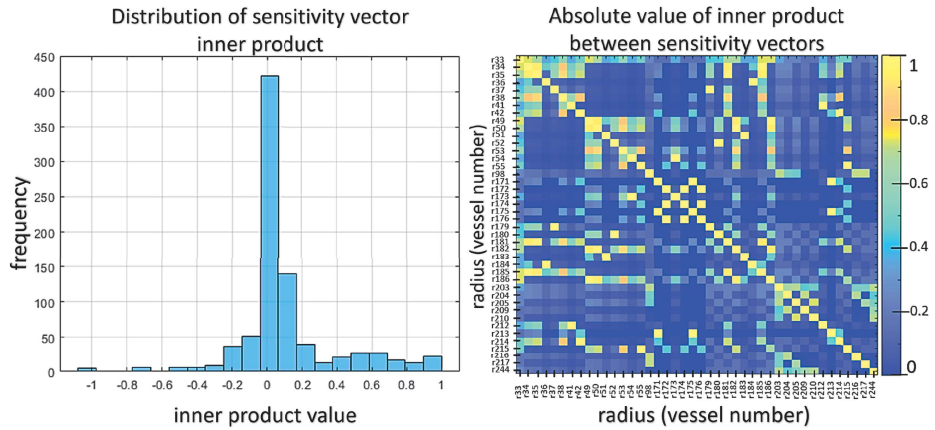


**Fig. 4.** Distribution of inner product values (left) and absolute value of the inner product (right). Absolute values range from 0 to 1.

**Global sensitivity - Sobol Analysis:** Investigation of convergence in first-order indices and corresponding confidence values showed that, for small sample size (i.e.,  $n = \{1, 3\}$ ), many indices were negative and their confidence values were relatively large ( $\geq 1.0$ ). For  $n = 10$ , all indices were  $\geq -0.006$ . Corresponding confidence values were all  $\leq 0.12$  which indicates relatively good convergence.

The matrix of first-order indices for this sample size and corresponding confidence matrix are shown in Fig. 5. Both show similar patterns, with visible symmetry between left and right leg.

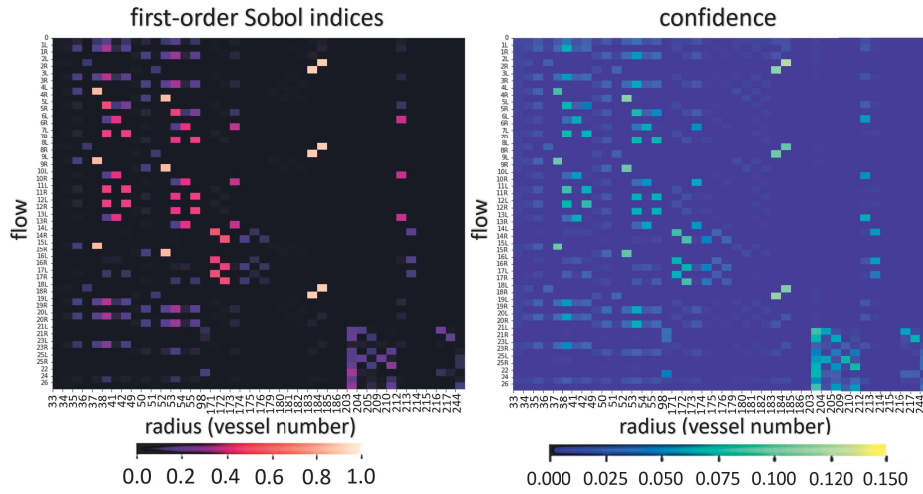


**Fig. 5.** Sobol indices of first order interactions between inputs and outputs (left) and corresponding confidence values (right). The colour scales are adjusted such that distinctive features of both matrices are visible.

Ranked sensitivity for flow  $Q_{20L}$  extracted from the matrix of first-order Sobol indices is shown in Fig. 6. The first five input parameters are the same as those identified using the local sensitivity analysis, although they appear in a different order.

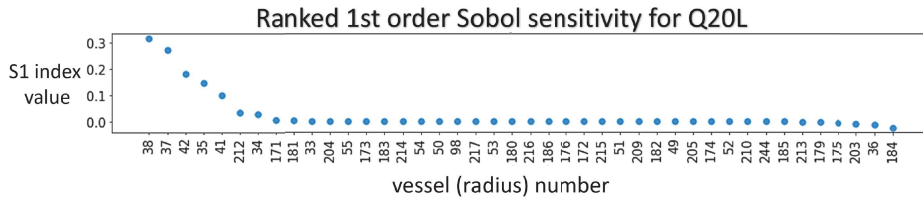


**Fig. 6.** Relative influence of input parameters (vessel radius) on  $Q_{20L}$  flow based on 1<sup>st</sup> order Sobol indices.

Second-order indices generally contributed less to the output variance with values ranging from  $-0.06$  to  $0.20$  with over 99% of these values being smaller than  $0.10$ . Confidence values of S2 ranged between  $0.0$  and  $0.12$  with 97% lower than  $0.05$ . An example of the matrix of second-order indices for output flow  $Q_{20L}$  is shown in Fig. 7.

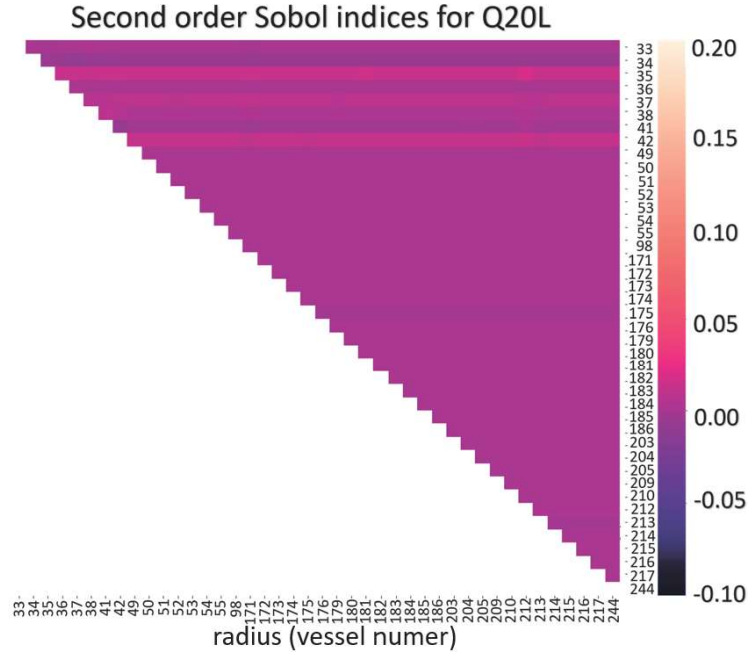


**Fig. 7.** Second order interactions between input parameters for flow  $Q_{20L}$ . Interactions of a parameter with itself and duplicate interactions are excluded.

**Influence of thrombus formation:** The difference in absolute sensitivity between the no-thrombus sensitivity and the 30% and 60% thrombosis cases is shown in Fig. 8. The higher the degree of thrombosis, the bigger the difference in absolute sensitivity. This is observed for the flows of the left leg, marked by a red frame in the plot, and for the output flow  $Q_{24}$  in the *inferior vena cava*. These results demonstrate that sensitivity of the system is dominated by the effects of the thrombus when the reduction of the vessel lumen is  $\geq 40\%$  while *anatomical* variation is 10%.

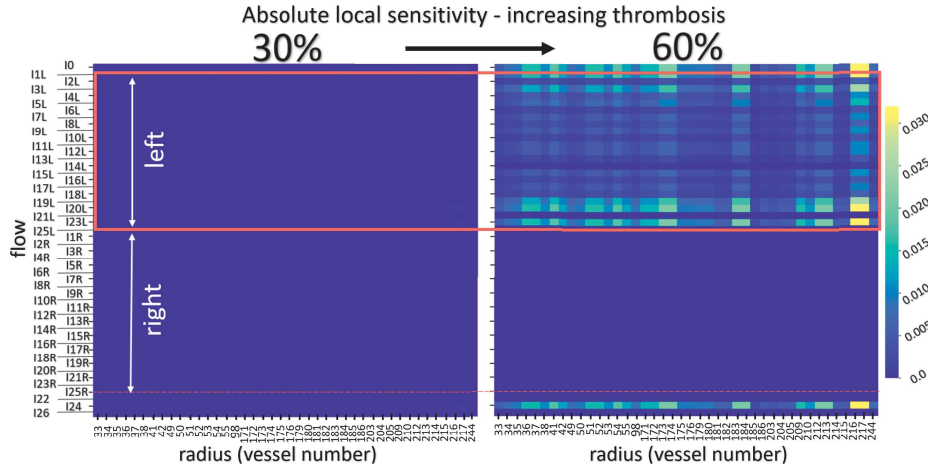


**Fig. 8.** Difference between absolute local sensitivity matrix for no-thrombosis case and two different degrees of thrombosis in the left common iliac vein. “Left” and “right” refer to legs.

## 4 Discussion

The focus of this study is on the assessment of the influence of anatomical variability on the distribution of flow within a model of the lower limb circulation with model parameters taken from Müller and Toro [7]. The sensitivity analyses reported here are an important step in examining the behaviour of the model, prior to further development including personalisation with clinical data, as discussed in detail by Huberts et al. [9].

The comparison of absolute and normalised sensitivity provided in Fig. 2 highlights the effect of variation of radii on the flow observed within the network. Both output measures provide useful information about the system and it is reasonable that the largest normalised change in flow is observed in locations associated with the venous return, as the flow in these vessels results from flow through all other vessels in the network.

The ranking of input parameters provided by the results shown in Fig. 3 is useful when the focus of the model operation is on predicting the flow in a specific location in the network (in this example the left common iliac vein). If such a model is personalised using clinical measurements of vascular anatomy then this ranking can be used to identify the most important radii for direct measurement and reduce the effort in assessing vasculature which has a small effect on the flow in the location of interest. Fig. 3 suggests such an approach is likely to be feasible for the current network, as relatively few input parameters are associated with higher sensitivity values for this specific model output.

The visualisation of orthogonal sensitivity of the model input parameters shown in Fig. 4 has the potential to inform approaches to reduce the complexity of the model. Although this is not necessary in the current model, due to low

computational cost (a single operation of the model takes less than a second), it may provide advantages in terms of both interpretation of the model behaviour and efficiency of model personalisation (by reducing the dimension of the search space). However, some care is required in interpretation of Fig. 4 as the approach taken here assigns the same significance to all model outputs. For specific clinical applications this may not be appropriate, as some model outputs will inform the detail of haemodynamics associated with patient outcomes more than others.

The global sensitivity analysis performed in this study was used to assess the contribution to variation of flow within the network over a wider range of radii values. Comparison of the magnitude of the first and second terms confirmed that interactions between input radii made a relatively small contribution to the variance in the output flows. It is notable that input radii which contributed the most to variation in a particular output flow were fairly consistently reported using both the local and global approach to assess sensitivity of the network (Fig. 3 and Fig. 6).

The results provided in Fig. 8 demonstrate the significance of the occlusion of a vessel due to the formation of a thrombus. Although thrombus formation is represented in the same manner as variation in anatomy, by varying the vessel radius, it is worth noting that this variation is of a larger range than that assumed for anatomical variation. The figure shows an increase in absolute sensitivity in the leg affected by the thrombosis. Changes in relative sensitivity were also observed, but only became significant for thrombosis greater than 60%.

## 5 Conclusion

This study demonstrates the value of local and global sensitivity analysis to inform development of a model of lower limb haemodynamics. The results obtained can be used to inform model reduction strategies and target clinical data collection, to maximise the accuracy of model estimates of flow in venous regions, prone to thrombus development. A suitably refined and parameterised model has clear potential to guide clinical decision-making by providing information beyond the level typically measured during patient follow-up.

## Acknowledgements

This publication is supported by the European Union’s Horizon 2020 research and innovation programme under grant agreement Sano No 857533 and carried out within the International Research Agendas programme of the Foundation for Polish Science, co-financed by the European Union under the European Regional Development Fund.

## References

1. Stone, J.: Deep vein thrombosis: pathogenesis, diagnosis, and medical management. *Cardiovascular Diagnosis and Therapy* **7**(3), 276-284 (2017)
2. Baldwin, M.J.: Post-thrombotic syndrome: a clinical review. *Journal of Thrombosis and Haemostasis* **11**(5), 795–805 (2013)
3. Beckman, M.G.: Venous thromboembolism: a public health concern. *American Journal of Preventive Medicine* **38**(4), 495-501 (2010)
4. Lim, C.S et al.: A centralised complex venous service model in an NHS hospital. *British Journal of Healthcare Management* **26**(2), 2-15 (2022)
5. Black, S.A. et al.: Management of acute and chronic iliofemoral venous outflow obstruction: a multidisciplinary team consensus. *International Angiology* **39**(1), 3-16 (2020)
6. Shi, Y. et al.: Review of Zero-D and 1-D Models of Blood Flow in the Cardiovascular System. *BioMedical Engineering OnLine* **10**:33 (2011)
7. Müller, L.O. and Toro, E.F.: A global multiscale mathematical model for the human circulation with emphasis on the venous system. *Int. J. Numer. Meth. Biomed. Engng.* **30**, 681-725 (2014)
8. Keijsers, J.M. et al.: A 1D pulse wave propagation model of the hemodynamics of calf muscle pump function. *Int J Numer Method Biomed Eng.* **31**(7), e02716 (2015)
9. Huberts, W. et al.: What is needed to make cardiovascular models suitable for clinical decision support? A viewpoint paper. *J Comp Sci.* **24**, 68-84 (2018)
10. Benemerito, I. et al.: Determining Clinically-Viable Biomarkers for Ischaemic Stroke Through a Mechanistic and Machine Learning Approach. *Ann Biomed Eng* (2022). <https://doi.org/10.1007/s10439-022-02956-7>
11. Li, R. et al.: Selection of model parameters for off-line parameter estimation. *IEEE Transactions on Control Systems Technology.* **12**(3), pp402 (2004)
12. Saltelli, A. et al.: Variance based sensitivity analysis of model output. Design and estimator for the total sensitivity index. *Computer Physics Communications.* **181**(2), 259-270 (2010)
13. Hose, D.R. et al.: Cardiovascular Models for Personalised Medicine: Where Now and Where Next? *Medical Engineering Physics,* **72**, 38-48 (2019)